L M M Auger spectra of selenium and some of its compounds

M. K. Bahl, R. L. Watson, and K. J. Irgolic

Citation: The Journal of Chemical Physics **72**, 4069 (1980); doi: 10.1063/1.439634
View online: http://dx.doi.org/10.1063/1.439634
View Table of Contents: http://scitation.aip.org/content/aip/journal/jcp/72/7?ver=pdfcov
Published by the AIP Publishing

LMM Auger spectra of selenium and some of its compounds[a)]

M. K. Bahl,[b)] R. L. Watson, and K. J. Irgolic

Department of Chemistry and Cyclotron Institute, Texas A&M University, College Station, Texas 77843
(Received 3 April 1979; accepted 12 December 1979)

The energies of the 3*s*, $3p_{3/2,1/2}$, and 3*d* photopeaks, and of the $L_{2,3}$ *MM* Auger peaks have been measured for selenium metal and some of its compounds. The associated relaxation energies were computed by two different methods; first by comparing the measured binding energies with those calculated theoretically employing Koopmans theorem, and second, by a method devised by Shirley and co-workers. The merits of these two methods are examined by comparing measured *LMM* and *LMN* Auger energies with those calculated using the predicted relaxation energies. The relative intensities of various Auger multiplets are compared with theoretical values for *L–S* and intermediate coupling of the final hole states.

I. INTRODUCTION

Current efforts to understand the effect of relaxation energy on the apparent binding energy of core levels have led to intensified interest in systematic studies of high resolution Auger spectra of various elements and their compounds. Earlier theoretical and experimental studies[1–3] on *LMM* Auger spectra of 3*d* transition metals have indicated that a satisfactory assignment of the structure can be made by considering the problem on an atomic scale. Robert *et al.*[4,5] have recently performed transition probability calculations for the $L_{2,3}MM$ Auger spectra of selenium and copper. However, no attempt was made in this work to resolve the various components of the $L_{2,3}MM$ Auger spectra of selenium, and hence a detailed comparison of the experimental intensities of various multiplets with the theoretical values could not be made.

We report here on measurements of core level binding energies and *LMM* Auger transition energies in selenium metal and some of its compounds. The binding energies are compared with those calculated theoretically using nonrelativistic Hartree–Fock and relativistic Dirac–Fock calculations. The contributions of atomic and extra-atomic relaxation to the binding energies of various levels of selenium are found from this comparison and also from the approximations put forward by Shirley[6,7] and Ley *et al.*[8] The magnitudes of atomic and extra-atomic relaxation thus found for $M_{4,5}$ levels are utilized to calculate the Auger energies for $L_{2,3}M_{4,5}M_{4,5}$ transitions using *L–S* and intermediate coupling for the two-hole final states. These theoretical values are compared with the experimental values. The intensities of various multiplets in the Auger spectrum of selenium metal were found to be in fair agreement with the theoretical calculations using intermediate coupling for the final two-hole states.

II. EXPERIMENTAL

The measurements were performed using a Hewlett–Packard 5950A ESCA spectrometer as described earlier.[9] A long-range scan of the region of interest for selenium metal is shown in Fig. 1. Most of the spectrum is dominated by the *LMM* Auger lines, whereas the selenium 3*s*, 3*p*, 3*d*, and valence band peaks are clearly visible in the low binding energy region of the spectrum. The features labeled *P* in Fig. 1 are thought to be due to plasmon excitation.

The samples were prepared either by vacuum evaporation or they were powdered and dispersed on gold-coated aluminum plates having striated surfaces. Some samples were taken in the form of thin strips after being cleaved from larger pieces. In the cases of the evaporated or cleaved samples, energies were measured relative to the Au $4f_{7/2}$ line originating from a small Au spot evaporated onto the surface of the sample. The energy of this line was taken to be 84.0 eV. Energies for the powdered samples were measured relative to the C 1*s* line, which could be observed as a result of contamination. The carbon 1*s* energy was measured relative to the Au $4f_{7/2}$ line in an evaporated Se metal sample and found to be 285.0 ± 0.1 eV.

III. CORE LEVEL SPECTRA

The core level binding energies for selenium metal obtained in the present study are listed in the second column of Table I. Also given in this table are binding energies from the work of Malmsten *et al.*,[10] Weightman

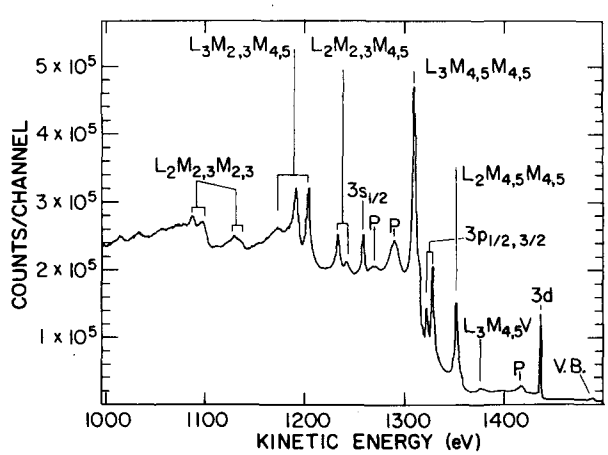

FIG. 1. XPS spectrum of selenium metal showing the *LMM* Auger structure.

a) This work was supported by the Robert A. Welch Foundation, The Texas A & M Center for Energy and Mineral Resources, and NSF Equipment Grant No. GP-41536.
b) Present address: The Technological Institute, Department of Materials Science and Engineering, Northwestern University, Evanston, Illinois 60201.

 0021-9606/80/074069-09$01.00

TABLE I. Core level binding energies, full width at half-maximum and relative intensities for selenium metal.

Level	Binding energy: Present work (±0.2 eV)	Malmsten *et al.*[a] (±0.6 eV)	Weightman *et al.*[b] (±1.0 eV)	Bearden and Burr[c]	Width: Present work	Shalvoy *et al.*[d]	Relative intensity	Experiment	Scofield[e]
$3s$	231.0	230.5	231.6	231.5±0.7	2.9±0.1		$\frac{3d_{5/2}}{3d_{3/2}}$	1.35±0.01	1.46
$3p_{1/2}$	167.7	167.4	168.5	168.2±1.3	2.1±0.1	2.5			
$3p_{3/2}$	161.9	161.7	162.6	161.9±1.0		2.8	$\frac{3p_{3/2}}{3p_{1/2}}$	2.63±0.01	1.93
$3d_{3/2}$	55.9				0.80±0.05		$\frac{3s}{3p_{1/2,3/2}}$	0.42±0.03	0.32
$3d_{av}$	55.5	55.5	56.4	56.7±0.8		1.8			
$3d_{5/2}$	55.1				0.80±0.05				

[a]Reference 10.
[b]Reference 11.
[c]Reference 12.
[d]Reference 39.
[e]Reference 14.

et al.,[11] and from the compilation of Bearden and Burr.[12] The present values are in good agreement with the Malmsten *et al.* values, while the Weightman *et al.* and the Bearden and Burr values are somewhat higher than ours. However, all the values in Table I agree within the stated experimental errors. Free-atom relativistic Dirac–Fock calculations[13] give the value of spin-orbit splitting for the $3d$, $3p$, and $2p$ levels (Table II) to be higher than the experimental values. The difference between the experimental and theoretical values amount to 20%, 8%, and 4.3% for the $3d$, $3p$, and $2p$ levels, respectively.

Table I also shows the full width at half-maximum and the relative intensity of each of the various photopeaks observed in selenium metal. The widths of the $3p$ and $3d$ photopeaks observed in the present studies with monochromatized Al $K\alpha_{1,2}$ radiation are much narrower than those obtained using unmonochromatized Al $K\alpha_{1,2}$ radiation. In fact, the $3d_{3/2,5/2}$ doublet is not even resolvable without monochromatization. The experimental relative intensity ratios are, for the most part, considerably different than those calculated theoretically by Scofield.[14] This is in contrast to observations on Te metal[15] where the experimental intensity

TABLE II. Comparison of experimental binding energies for selenium with those calculated for an isolated selenium atom (all values are in eV).

Level	Experimental values	Values from optical and x-ray spectra	$-E_{HF}$[b]	$-E_{RDF}$[c]	e_{rel}	Relaxation energies: Method I R	Method I R_a	Method I R_{ex}	Method II R	Method II R_a	Method II R_{ex}
$1s$	12657.0[a]	12660.4	12535.2	12739.2	204.0	82.2	51.5	30.7	63.8	55.4	8.4
$2s$	1654.8[a]	1657.7	1645.8	1692.0	46.2	37.2	26.4	10.8	36.3	28.2	8.1
$2p_{1/2}$	1475.0[a]	1478.5		1510.9		35.9					
$2p_{av}$	1454.8	1458.2	1471.7	1489.8	18.1	35.0	28.7	6.3	37.0	28.8	8.2
$2p_{3/2}$	1434.6	1438.0		1468.7		34.1					
$3s$	231.0	233.6	238.1	245.8	7.7	14.8	8.2	6.6	11.3	3.6	7.7
$3p_{1/2}$	167.7	170.8		182.2		14.5					
$3p_{av}$	164.8	167.7	176.3	179.1	2.8	14.3	8.4	5.9	11.4	3.7	7.7
$3p_{3/2}$	161.9	164.5		175.9		14.0					
$3d_{3/2}$	55.9	59.3		66.2		10.4					
$3d_{av}$	55.5	58.9	67.1	65.7	−1.4	10.2	8.3	1.9	11.4	3.7	7.7
$3d_{5/2}$	55.1	58.5		65.2		10.1					
$4s$	15.1	17.1	17.8	18.4	0.6	3.3	1.1	2.2	6.4	0	6.4
$4p_{1/2}$	5.6			5.8							
$4p_{av}$	4.1		5.6	5.6	0	1.4	0.7	0.7	5.8	0	5.8
$4p_{3/2}$	2.6	4.7		5.4							

[a]Computed using x-ray energies from Ref. 40 and binding energies of other levels measured in the present work.
[b]Hartree–Fock orbital eigenvalues.
[c]Relativistic Dirac–Fock orbital eigenvalues from Ref. 13.

ratios for the various peaks were found to be within 3% of the theoretical values. The large difference in the intensity ratio for $3p_{3/2}/3p_{1/2}$, to some extent, can be attributed to the uncertainty in the form of the background (Fig. 1). However, the difference in the intensity ratio for $3d_{5/2}/3d_{3/2}$ is difficult to understand.

In Table II, the present experimental binding energies are compared with the values for a free selenium atom as derived from optical data[16] and x-ray data.[12] An average difference of 2.9 eV between the present experimental values for selenium metal and those derived for a free selenium atom from optical and x-ray data may be noted. This energy difference should be equal to the extra-atomic relaxation energy. However, the average extra-atomic relaxation energy predicted by the calculations to be discussed below is considerably larger than the observed energy difference. This discrepancy may be attributed to the fact that electronic binding energies are smaller in metals than they are in free atoms, and the relative amounts by which they are reduced are greater for core levels than for outer levels.[17,18] Thus, free-atom x-ray energies will be systematically larger than those for metals. This will cause the selenium binding energies derived from optical plus x-ray data (for metals) to be smaller than they should be for free atoms.

The experimental binding energies for selenium metal are further compared with the results of free atom self-consistent field calculations in Table II. The fourth column of this table lists nonrelativistic Hartree–Fock orbital energies[19] $-E_i$, which are (according to Koopmans theorem) the energies that would be required to remove the various electrons if the rest of the electrons in the atom were not allowed to readjust (relax) to the final state potential. In order to estimate the changes in the binding energy introduced by relativity, column 5 gives the orbital eigenvalues obtained from fully relativistic Dirac–Fock calculations.[13] A work function value of 5.1 eV, as found by Schulze,[20] has been subtracted from both the optical and the theoretical energies. Column 6 lists the contribution of relativity to the binding energies of the various levels. As expected, the relativistic contributions to the inner shell binding energies are quite large.

Neglecting the effects of electron correlation, the total relaxation energy for a given level is presumed to be

$$R = -E_{\mathrm{RDF}} - E_{\mathrm{expt}} , \tag{1}$$

where E_{expt} is the experimental binding energy. These energy differences are listed in column 7 of Table II. The relaxation energy due to the readjustment of the orbitals in a free atom during photoemission (atomic relaxation) is just

$$R_a = -E_{\mathrm{RDF}} - \Delta E_{\mathrm{RDF}} , \tag{2}$$

where ΔE_{RDF} is the relativistic Dirac–Fock total energy difference between the final and initial states (i.e., $\Delta E = E_f - E_i$). Once the atomic relaxation contribution has been determined, the extra-atomic relaxation contribution may be obtained from the relation

TABLE III. Relaxation energies for various levels of selenium as computed from those for krypton.

Shell	Relaxation energy (eV)
$1s$	51.7
$2s$	24.4
$2p_{1/2}$	27.4
$2p_{3/2}$	26.8
$3s$	7.1
$3p_{1/2}$	7.4
$3p_{3/2}$	7.2
$3d_{3/2}$	7.5
$3d_{5/2}$	7.4
$4s$	0.5
$4p_{1/2}$	0.05
$4p_{3/2}$	−0.09

$$R_{ex} = R - R_a . \tag{3}$$

Unfortunately, the relativistic Dirac–Fock calculations needed to evaluate R_a have not yet been carried out for selenium. In the work reported here, we make use of approximate procedures. The nonrelativistic Hartree–Fock program of Froese-Fischer[19] has been used to evaluate ΔE in Eq. (2) for each orbital of Se. The resulting values of R_a are tabulated in column 8 of Table II. The error introduced due to neglect of relativistic effects in these calculations is expected to be small for all but the innermost ($1s$, $2s$, and $2p$) orbitals. Values of R_a for the various orbitals of selenium can also be estimated using the Dirac–Fock calculations of Rosen and Lindgren[21] for Kr by subtracting the contribution to the atomic relaxation made by the two extra $4p$ electrons of krypton. This quantity, in turn, can be estimated using the equivalent cores approximation and Mann's tables[22];

$$(\Delta R_{4p})_{\mathrm{Kr}} \simeq F^0(nl, 4p; \mathrm{Rb}) - F^0(nl, 4p; \mathrm{Kr}) . \tag{4}$$

The $F^0(nl, 4p)$ integral varies nonlinearly with atomic number and consequently the equivalent cores approximation produces a different value of the relaxation contribution of two $4p$ electrons when it is evaluated for Se;

$$(\Delta R_{4p})_{\mathrm{Se}} = [F^0(nl, 4p; \mathrm{Br}) - F^0(nl, 4p; \mathrm{Se})] . \tag{5}$$

Therefore it is reasonable to subtract the average of (4) and (5) from the values calculated for krypton. The values of relaxation energy obtained for the various orbitals by this method are tabulated in Table III. It is to be noted that these two methods yield relaxation energies which only differ by 1 to 2 eV.

Shirley[6,7] has devised another procedure for estimating atomic relaxation energies and a method for the estimation of extra-atomic relaxation energies in metals has been discussed by Kowalczyk *et al.* and by Ley *et al.*[8] We have previously applied this method to the calculation of relaxation energies for tellurium and the details of the procedure employed are given in Ref. 23.

The relaxation energies predicted by these methods were calculated using Mann's tables of F and G integrals, and the integral coefficients given by Shirley.[6] They are listed in columns 9, 10, and 11 of Table II under the heading Method II. It is seen that the values obtained

for the total relaxation energy R, by both methods are in fair agreement except for the $1s$, $3p$, $3s$, $4s$, and $4p$ levels. The discrepancy in the case of the $3s$ and $3p$ levels may be due to the neglect of intra-shell relaxation in Method II. In general, however, the agreement between the atomic and extra-atomic contributions is quite poor, with the maximum discrepancy occurring for the $1s$ levels. It may be further noted that, whereas the value of the extra-atomic relaxation energy derived by Method II for the $1s$ level is not very much different than for the other levels, the $1s$ value calculated by the Hartree–Fock method differs considerably from the others. This was also the case for the Te $1s$ and $2p$ levels as reported in our earlier communication.[23] Moreover, it was shown that the relaxation energy computed by Method I for the Te $2p$ level was too large to account for the observed KLL Auger energies. To delineate the systematic behavior of this extra-atomic relaxation energy discrepancy, calculations were performed for a number of other elements. Figure 2(a) shows the relaxation energy difference as a function of atomic number and Fig. 2(b) shows the relaxation energy difference as a function of the relativistic contribution to the $1s$ level. The increase in the discrepancy (which is equivalent to only a 0.2% error in the orbital eigenvalue) with Z and with relativistic correction, respectively, suggests that the problem may simply reflect the limits of accuracy of methods employed in the relativistic Dirac–Fock calculations.

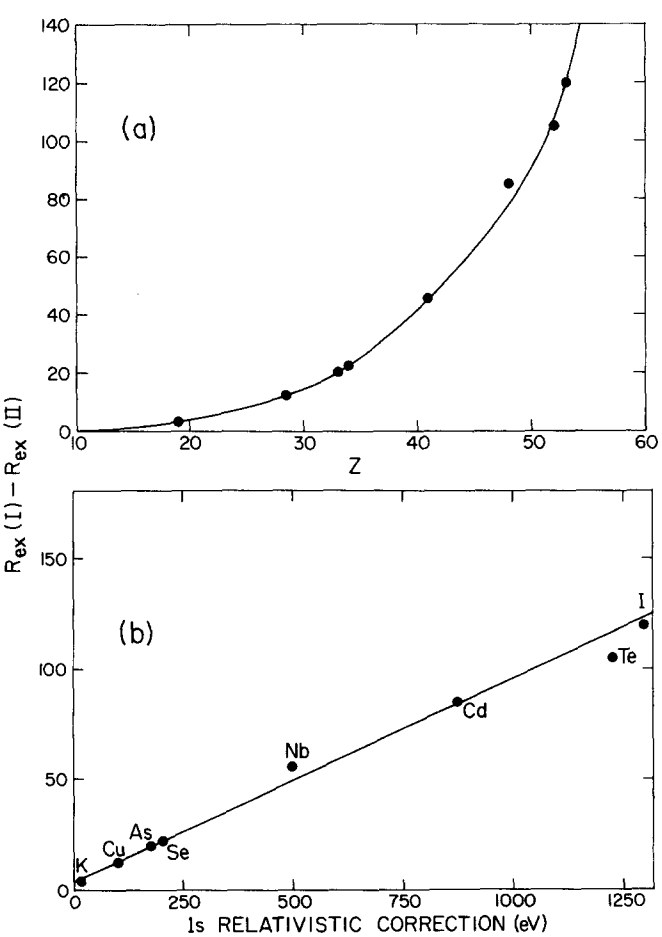

FIG. 2. Difference in the $1s$ extra-atomic relaxation energies calculated by Methods I and II as a function of (a) atomic number and (b) relativistic energy correction for the $1s$ level.

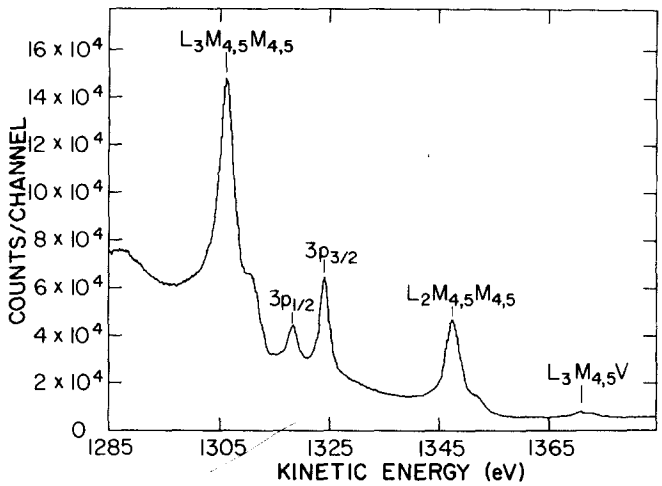

FIG. 3. $L_{2,3}MM$ Auger spectrum of selenium metal.

IV. *LMM* AUGER SPECTRA

The $L_{2,3}MM$ Auger spectrum of selenium metal is shown in Fig. 3. The various complex peaks appearing in the L_3MM and L_2MM Auger structures were resolved by means of a least-squares program employing a Gaussian–plus–exponential tail fitting function. The resolved structure for the $L_3M_{4,5}M_{4,5}$ and $L_2M_{4,5}M_{4,5}$ Auger peaks are shown in Fig. 4. We here report on the analysis of the Auger $L_{2,3}M_{4,5}M_{4,5}$ spectrum in terms of LS coupling with the inclusion of the diagonal spin–orbit matrix elements, and in terms of intermediate coupling.

A. Multiplet intensities and energies

Auger transition rates for $L_{2,3}MM$ and MNN lines have, have, in the past been treated using jj coupling for the initial inner shell and continuum vacancies and LS coupling or intermediate coupling (IC) for the two holes in the final state. Such a mixed-coupling scheme was first applied by Asaad and Melhorn[24] to the $L_{2,3}MM$ spectrum of argon and later by El Ibyrari *et al.*[25] and Hagmann *et al.*[26] to the $M_{4,5}NN$ spectrum of xenon. It was found in these later studies that the use of intermediate coupling considerably improved the agreement between theory and experiment over that attained with L–S coupling.

In the present work, the intensities of the various $L_{2,3}MM$ multiplets in the Auger spectrum of selenium were calculated using L–S coupling and intermediate coupling. The transition rates for L–S coupling were obtained by solving the expression given by El Ibyari *et al.*[25] using values for the various direct and exchange integrals as calculated by McGuire[27] for $Z = 34$. The transition rates for intermediate coupling were calculated following the procedure outlined by Hagmann *et al.*[26] as described in our previous work on Te Auger structure.[28]

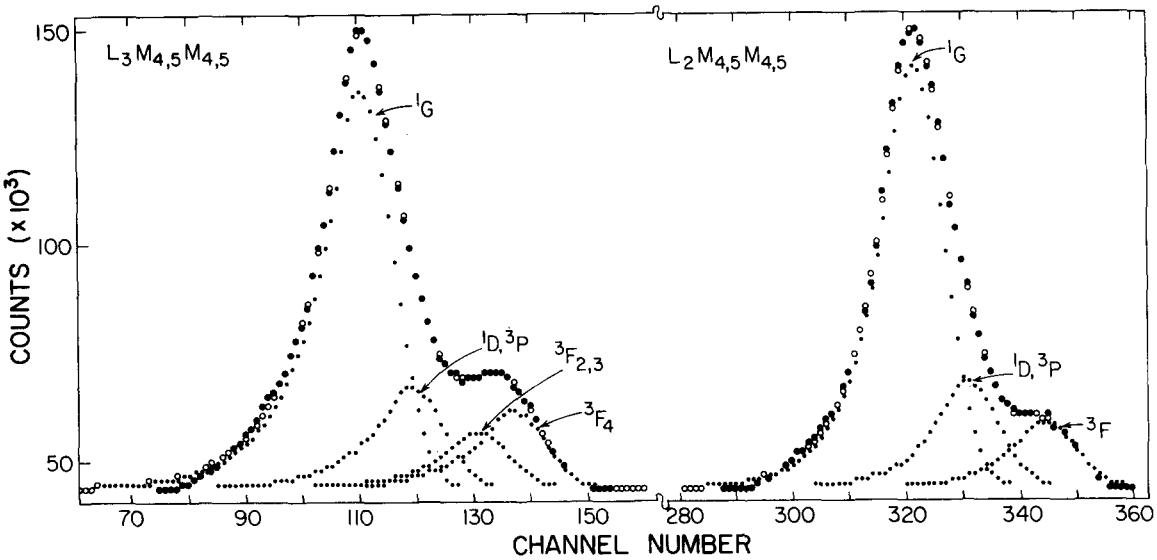

FIG. 4. Fitted $L_{2,3}MM$ Auger spectrum of selenium metal showing the various multiplet components. The closed circles represent the data points and the open circles show the calculated spectrum.

The experimental intensities of the various resolved Auger peaks for selenium metal are compared with the corresponding theoretical intensities in Table IV. It is seen that the experimental intensities for selenium metal agree closely with the IC predictions. Relative energies of various multiplets calculated using L–S coupling and intermediate coupling for the final two-hole states are tabulated in Table V. The spin–orbit diagonal elements have been included in the L–S coupling scheme. A comparison between the experimental and the theoretical line energies shows that the observed energy splittings agree fairly well with those calculated using intermediate coupling. However, it may be noted that the observed energy splitting is generally smaller than that obtained from theory. Similar trends have been noted in the Auger spectra of zinc[29] and cadmium metals.[30]

TABLE IV. Experimental and theoretical relative intensities of the $L_{2,3}M_{4,5}M_{4,5}$ Auger diagram lines for Se metal.

Transition	Multiplets	L–S coupling	Intermediate coupling		Experimental
$L_2M_{4,5}M_{4,5}$	$^3F_4$	7.5	5.2		
	$^3F_3$	8.4	8.4	18.0	11.4
	$^3F_2$	7.4	4.4		
	$^1D_2$	10.9	9.0		
	$^3P_2$	0.6	5.5	15.8	17.7
	$^3P_1$	1.0	1.0		
	$^3P_0$	0.5	0.3		
	$^1G_4$	61.9	64.3		70.9
	$^1S_0$	1.8	2.0		
$L_3M_{4,5}M_{4,5}$	$^3F_4$	11.2	12.5		12.0
	$^3F_3$	7.4	7.3	13.6	8.9
	$^3F_2$	4.6	6.3		
	$^1D_2$	10.9	6.9		
	$^3P_2$	1.5	3.5	11.1	15.8
	$^3P_1$	0.5	0.5		
	$^3P_0$	0.1	0.2		
	$^1G_4$	61.9	61.1		63.3
	$^1S_0$	1.8	1.7		

B. Relative L_2 and L_3 subshell transition intensities

It is interesting to compare the relative intensities of the $L_{2,3}M_{4,5}M_{4,5}$ Auger transitions with the relative intensities of the L_2 and L_3 photopeaks and with the photoionization cross sections calculated for the L_2 and L_3 subshells by Scofield.[14] Such a comparison is given in Table VI for Zn and Cu (estimated from the data of Kowalczyk *et al.*[1]), for As (from the data of Bahl *et al.*[9]), and for Se (from the present data and from the data of Weightman *et al.*[31]); also, the value of the $L_3M_{4,5}M_{4,5}/L_2M_{4,5}M_{4,5}$ intensity ratio for selenium metal obtained in the present investigation (using monochromatized Al $K\alpha_{1,2}$ radiation) is found to be quite different from that obtained by Weightman *et al.*,[31] who used unmonochromatized Al $K\alpha_{1,2}$ radiation.

The large difference between the $L_3M_{4,5}M_{4,5}/L_2M_{4,5}M_{4,5}$ Auger intensity ratio and the $2p_{3/2}/2p_{1/2}$ photoionization cross section ratio for copper is well understood and is attributed to the transfer of L_2 holes to the L_3 subshell via L_2L_3X Coster–Kronig transitions. This is consistent with the theoretical results of Chen *et al.*[32] which

TABLE V. Experimental and theoretical energies of $L_{2,3}M_{4,5}M_{4,5}$ Auger diagram lines in selenium relative to the $^1G_4$ energy.

			Experimental values (eV)	
Multiplet	L–S coupling	I–C coupling	$L_3M_{4,5}M_{4,5}$ (± 0.05 eV)	$L_2M_{4,5}M_{4,5}$ (± 0.1 eV)
$^3F_4$	5.4	5.5	5.2	
$^3F_3$	4.8	4.8	4.0	4.6
$^3F_2$	4.3	4.4		
$^1D_2$	1.8	2.0	1.7	1.9
$^3P_2$	1.3	1.0		
$^3P_1$	1.0	1.0		
$^3P_0$	0.8	0.9		
$^1G_4$	0	0	0	0
$^1S_0$	−7.3	−7.4		

TABLE VI. Auger and photopeak intensity ratios and photoionization cross section ratios for L_2 and L_3 electrons.

Element	$L_3M_{4,5}M_{4,5}/L_2M_{4,5}M_{4,5}$ Auger	$2p_{3/2}/2p_{1/2}$ photopeak	$\sigma_{2p_{3/2}}/\sigma_{2p_{1/2}}$ [a]
Cu	4.8[b]	2.0[b]	1.93
Zn	2.3[b]	2.0[b]	1.93
As	2.8[c]	2.9[c]	1.93
Se	3.35[d]		2.12
	2.3[e]		

[a]Theoretical photoionization cross section ratios from Ref. 14.
[b]Estimated from spectra given in Ref. 1.
[c]From Ref. 9.
[d]Present work.
[e]From Ref. 31.

indicate that the L_2L_3X Coster–Kronig transition probability is fairly large in Cu. In Zn, on the other hand, L_2L_3X Coster–Kronig transitions are not energetically possible, and hence the Auger, photopeak, and photoionization cross section ratios are nearly the same.

With monochromatic Al $K\alpha$ x rays, holes are not produced in the L_1 subshells of As and Se because the L_1 binding energy is greater than the Al $K\alpha$ x-ray energy. Moreover, the L_2L_3X Coster–Kronig transition probabilities are predicted to be small for As and Se. One should therefore expect the three ratios (Auger, photopeak, and photoionization cross section) to be about the same for As and Se also. Although there is close agreement between the Auger and photopeak intensity ratios for As, it is apparent from Table IV that the photoionization cross section ratio deviates significantly from the two intensity ratios. In the case of selenium, the $2p_{1/2}$ binding energy is close to the Al $K\alpha_{1,2}$ energy and threshold effects can alter the photoionization cross sections. In a forthcoming paper, we will discuss how the Auger intensity ratio changes as a function of the chemical shifts of the core levels.[33]

It is surprising to find that the $L_3M_{4,5}M_{4,5}/L_2M_{4,5}M_{4,5}$ Auger intensity ratio for selenium is smaller with unmonochromatized than with monochromatized Al $K\alpha_{1,2}$ radiation. Because of contributions to the production of L_3 holes from L_1L_3X Coster–Kronig transitions resulting from L_1 photoionization which occurs when unmonochromatized Al $K\alpha_{1,2}$ radiation is used, one would expect to obtain a smaller Auger intensity ratio with monochromatized Al $K\alpha_{1,2}$ radiation, with which L_1 photoionization cannot cocur. This experimental observation seems to indicate that the $2p_{3/2}/2p_{1/2}$ photoionization cross section ratio is considerably different in the two cases.

C. Relaxation energies

As a means of checking the total relaxation energies obtained in Sec. III, the absolute energy positions of the various Auger multiplets were determined. Shirley[1] has shown that the Auger transition energy is accurately given by the expression.

$$E_{ijk}(x) = E_i - E_j - E_k - f_{ijk}(x) + R_s \ . \qquad (6)$$

Here the E_n's are one-electron binding energies, $f(x)$ is the two-electron interaction energy for final state x, and R_s is the (static) relaxation energy. The relaxation energy R_s is the amount by which the binding energy of electron k is decreased due to the relaxation of the system following the ejection of electron j. Hedin and Johansson[34] have shown that $R_s \simeq 2R$.

The measured Auger electron energies are listed in Table VII where they are compared with the experimental energies of Robert *et al.*[4] and with the energies calculated from Eq. (6) using the values of R obtained by methods I and II (Table II). In general, the theoretical values are lower than the experimental values. However, the agreement is better using the relaxation energies given by Method II than using these obtained with Method I.

In the above discussion, the relaxation energy for the Auger transition was calculated under the assumption that the atomic as well as the extra-atomic relaxation energy does not depend on whether or not the shell from which the electron is ejected has already lost an electron. However, recently Hoogewigs *et al.*[35] have shown that the relaxation energy of a shell with a hole and without a hole can differ by a few eV. To take this into account, the total relaxation energy appearing in Eq. (6) may be written

$$R_s = R(jk) + \Delta E_R(k) \ ,$$

where the additional term $\Delta E_R(k)$ represents the increase in the relaxation energy of the k shell in the presence of a j hole. Hoogewigs *et al.*[35] have estimated R_s for selenium using optimized HFS hole state calculations and obtained a value of 27.8 eV for the $(3d, 3d)$ hole state. However, the value of 27.8 eV for the total relaxation energy does not give better agreement with the experimental values than that obtained by Method II.

TABLE VII. Auger (kinetic) energies for selenium metal.

Auger transition	Final state term	Calculated energies (eV) Method I	Method II	Experimental energies (eV)
$L_2M_{4,5}M_{4,5}$	$^3F_4$	1348.3	1350.7	
	$^3F_3$	1347.6	1350.0	1352.8
	$^3F_2$	1347.2	1349.6	
	$^1D_2$	1344.8	1347.2	1350.1
	$^3P_2$	1343.8	1346.2	
	$^3P_1$	1343.8	1346.2	
	$^3P_0$	1343.7	1346.1	
	$^1G_4$	1342.8	1345.2	1348.2
	$^1S_0$	1335.4	1337.8	
$L_3M_{4,5}M_{4,5}$	$^3F_4$	1307.8	1310.2	1312.2
	$^3F_3$	1307.1	1309.5	1311.0
	$^3F_2$	1306.7	1309.1	
	$^1D_2$	1304.3	1306.7	1308.7
	$^3P_2$	1303.3	1305.7	
	$^3P_1$	1303.3	1305.7	
	$^3P_0$	1303.2	1305.6	
	$^1G_4$	1302.3	1304.7	1307.0
	$^1S_0$	1294.0	1297.3	
$L_3M_{4,5}N_2$		1364.6	1374.8	1371.5
$L_3M_{4,5}N_3$		1367.6	1377.8	1375.1

TABLE VIII. Theoretical and experimental energies of $L_{2,3}M_{4,5}M_{4,5}$ Auger diagram lines in selenium compounds relative to the $^1G_0$ energy.

Transitions	Multiplets	Theoretical values—IC	Se metal (±0.05)	$FeSe_2$ (±0.05)	$MoSe_2$ (±0.05)	Bi_2Se_3 (±0.6)	$CuSe_2$ (±0.05)	As_2Se_3 (±0.05)	Cu_2Se (±0.05)	Nb_3Se_4 (±0.1)
$L_2M_{4,5}M_{4,5}$	$^3F_4$	5.5		5.4		5.2				
	$^3F_3$	4.8	4.6	4.3	4.6	4.1	4.6	4.8		4.8
	$^3F_2$	4.4								
	$^1D_2$	2.0	1.9	1.8	1.9	1.9	2.1	1.9		2.2
	$^3P_2$	1.0								
	$^3P_1$	1.0								
	$^3P_0$	0.9								
	$^1G_0$	0	0	0	0	0	0	0		0
	$^1S_0$	−7.4		−6.3		6.7				
$L_3M_{4,5}M_{4,5}$	$^3F_4$	5.5	5.2	5.2	5.2					
	$^3F_3$	4.8	4.0	4.1	4.1	4.8	4.8	4.8	4.9	4.8
	$^3F_2$	4.4								
	$^1D_2$	2.0	1.7	1.7	1.8	2.3	2.4	2.1	2.5	2.3
	$^3P_2$	1.0								
	$^3P_1$	1.0								
	$^3P_0$	0.9								
	$^1G_0$	0	0	0	0	0	0	0	0	0
	$^1S_0$	−7.4		−6.6	6.4	6.3				

In an effort to distinguish which method more accurately predicts the extra-atomic relaxation contribution to the total relaxation energy, measurements were carried out for the $L_3M_{4,5}N_{2,3}$ Auger transitions. Neglecting the small multiplet splitting for these two transitions, Eq. (6) gives

$$E(L_3M_{4,5}N_{2,3}) = E(L_3) - E(M_{4,5}) - E(N_{2,3}) - F_0(3d, 4p) + R_s(M_{4,5}N_{2,3}) ,$$

where the static relaxation energies are taken to be

$$R_s(M_{4,5}N_{2,3}) = 2[R_a(N_{2,3}) + R_{ex}(M_{4,5})] .$$

Since the atomic relaxation energy is very small for both of these cases (consisting only of intrashell contributions), almost the entire relaxation energy is associated with extra-atomic relaxation. Using the values of R_a and R_{ex} given in Table II,

	Method I	Method II
$R_s(M_{4,5}N_{2,3}) =$	5.2	15.4

In Table VII, the experimental Auger energies for the $L_3M_{4,5}N_{2,3}$ transitions are compared with these calculated as described above. It is seen that the energies computed by Method II give better agreement than the ones computed by Method I.

Recently, Larkins[36] has estimated extra-atomic re-

TABLE IX. Experimental and theoretical relative intensities of the $L_{2,3}M_{4,5}M_{4,5}$ Auger diagram lines for selenium compounds.

Transitions	Multiplets	Theoretical values—IC	Se metal	$FeSe_2$	$MoSe_2$	Bi_2Se_3	$CuSe_2$	As_2Se_3
$L_2M_{4,5}M_{4,5}$	$^3F_4$	5.2		5.3±0.6	13.1±1.0	6.0±0.5	11.8±0.06	
	$^3F_3$	8.4	11.5±1.0	8.8±1.0				
	$^3F_2$	4.4						
	$^1D_2$	9.0						
	$^3P_2$	5.5	15.8	17.9±1.0	17.6±1.0	19.8±0.5	18.2±0.8	15.0±1.0
	$^3P_1$	1.0						
	$^3P_0$	0.3						
	$^1G_4$	64.3	70.6±1.0	68.0±1.0	67.1±0.8	66.3±1.0	73.2±1.5	
	$^1S_0$	2.0		0.4±0.1		1.2±0.3		
$L_3M_{4,5}M_{4,5}$	$^3F_4$	12.5	12.0±1.0	12.8±0.4	12.5±0.6			
	$^3F_3$	7.3	8.9±0.5	9.0±0.6	9.0±0.6	19.2±1.0	17.1±1.0	19.7±1.0
	$^3F_2$	6.3						
	$^1D_2$	6.9						
	$^3P_2$	3.5	11.1	15.8±1.0	14.7±1.0	16.2±0.5	15.3±0.5	12.1±0.5	15.4±0.5
	$^3P_1$	0.5						
	$^3P_0$	0.2						
	$^1G_0$	61.1	63.3±1.0	63.0±1.0	62.3±1.0	64.9±1.5	70.8±2.0	64.9±1.0
	$^1S_0$	1.7		0.5±0.1	0.7±0.1	0.7±0.2		

TABLE X. Theoretical and experimental relative intensities of the $L_{2,3}M_{4,5}M_{4,5}$ Auger diagram lines in zinc.[a]

Transition	Multiplets	Theory (intermediate coupling)	Experiment
$L_2M_{4,5}M_{4,5}$	$^3F_{2,3,4}$	19.4	13.6
	$^1D_2$, $^3P_{0,1,2}$	13.9	14.8
	$^1G_4$	64.9	67.6
	$^1S_0$	1.8	4.0
$L_3M_{4,5}M_{4,5}$	$^3F_{2,3,4}$	23.3	23.7
	$^1D_2$, $^3P_{0,1,2}$	12.3	14.3
	$^1G_4$	62.8	60.1
	$^1S_0$	1.6	2.0

[a]From Ref. 38.

laxation energies in solids using an atomic Hartree–Fock screening model. He obtained the following expression for the extra-atomic relaxation energy:

$$(R_{ex})_s = 2n\langle \alpha X\rangle_{Z+1} - n^2\langle \alpha\alpha\rangle_{Z+1} , \quad (7)$$

where $\langle \alpha x\rangle_{Z+1}$ represents the interaction energy of electrons in the α and x orbitals of an atom having atomic number $Z+1$, $\langle \alpha\alpha\rangle_{Z+1}$ represents the interaction energy of a pair of electrons in the outermost orbital α of atom $Z+1$, and n is a screening parameter (0.6). Equation (7) gives $(R_{ex})_s = 9.6$ eV for selenium and using this value along with $(R_a)_s = 2R_a = 16.6$ eV from Table II (Method I) gives a total relaxation energy of 26.5 eV. Putting this value in Eq. (7), one obtains agreement between the experimental and theoretical $L_{2,3}M_{4,5}M_{4,5}$ Auger energies to within 1 eV.

D. Chemical effects on widths and relative intensities

It is often observed that Auger lines from solids exhibit shape and width variations. These phenomena are usually related to the chemical state and environment of the parent element, and are most pronounced for transitions between levels with the smallest binding energies (i.e,. valence band and other core shells). For example, Gallon and Nuttal[37] recently showed that the $M_{4,5}N_{4,5}N_{4,5}$ Auger lines from CdS are broader than those observed in cadmium metal.

To observe the effect of chemical bonding on the relative intensities and energies of various multiplets, some intermetallic compounds of selenium were studied.

TABLE XII. Total $L_3M_{4,5}M_{4,5}$ to $L_2M_{4,5}M_{4,5}$ Auger intensity ratios.

Compound	Selenium metal (±0.1)
Se metal	3.2
$FeSe_2$	2.7
As_2Se_3	3.2
$CuSe_2$	2.8
$MoSe_2$	2.4
Nb_3Se_4	3.3

Intermetallic compounds offer definite advantages over ordinary inorganic compounds in that they are not as susceptible to radiation damage and charging effects.

The measured relative energies and intensities of various $L_2M_{4,5}M_{4,5}$ and $L_3M_{4,5}M_{4,5}$ multiplet components are listed in Tables VIII and IX, respectively, for the different compounds. In general, the peak positions (measured relative to $^1G_4$) and relative intensities do not vary much from one compound to another. In view of the experimental resolution, the small variations in the intensities and energies do not permit a detailed discussion. However, certain systematic trends may be noted from Tables VIII and IX. In particular, the energy separations (Table IX) between the various multiplet components in the different compounds are in general smaller than the free atom values, in agreement with other studies on Zn,[29] and Cd.[30] It would be of interest to observe the multiplet structure under higher resolution for the purpose of comparing with that observed for an isolated selenium atom or in SeH_4. Moreover, in all the compounds, the observed intensities of the $^1G_4$ and the $^1D_2$–$^3P_{0,1,2}$ components are larger than the theoretical values, while those of the $^3F_{2,3}$ component are smaller. A similar trend was observed in the $L_2M_{4,5}M_{4,5}$ Auger spectrum of zinc vapors[28,37] as shown in Table X. It may be further noted from Table X that the multiplet intensity variations among the various compounds, display essentially the same pattern in both the $L_2M_{4,5}M_{4,5}$ and the $L_3M_{4,5}M_{4,5}$ Auger spectra.

The total relative intensity ratios and the average widths of the $L_3M_{4,5}M_{4,5}$ and $L_2M_{4,5}M_{4,5}$ Auger peaks are listed in Tables XI and XII, respectively. It is seen (Table XI) that except for Bi_2Si_3, the average peak width ratio in the two Auger spectra is close to unity, which further indicates the absence of L_2L_3X Coster–Kronig transitions. The average widths of the $L_3M_{4,5}M_{4,5}$ or

TABLE XI. Average widths of the $L_{2,3}M_{4,5}M_{4,5}$ Auger peaks observed in various selenium compounds. (All values in eV.)

Transitions	Se metal	$FeSe_2$	$MoSe_2$	Bi_2Se_3	$CuSe_2$	$NiSe_2$
$L_3M_{4,5}M_{4,5}$	2.66±0.04	2.31±0.07	2.02±0.08	2.30±0.08	2.45±0.05	2.78±0.08
$L_2M_{4,5}M_{4,5}$	2.52±0.04	2.43±0.07	1.85±0.05	2.00±0.06	2.36±0.05	2.70±0.07
$\frac{L_3M_{4,5}M_{4,5}}{L_2M_{4,5}M_{4,5}}$	1.06	0.95	1.09	1.15	1.04	1.03

$L_2M_{4,5}M_{4,5}$ lines relative to the width of any photopeak ($3p$ or $3d$) is maximum for selenium metal. This is in agreement with our earlier results on various tellurium compounds.[28] However, in the present investigation, no correlation was found between the average width of the Auger lines and the relaxation energy of the compound, as was the case in the tellurium study.

It is seen from Table XII that the $L_3M_{4,5}M_{4,5}$ to $L_2M_{4,5}M_{4,5}$ relative intensity ratio is greater than two in all the selenium compounds and varies significantly from one compound to another. Since the $2p_{1/2}$ core level of selenium is close to the energy of the Al $K\alpha_{1,2}$ radiation, this may be due to a threshold effect on the ionization cross sections.

[1]S. P. Kowalczyk, R. A. Pollack, F. R. McFeely, L. Ley, and D. A. Shirley, Phys. Rev. B 8, 2387 (1973).
[2]E. J. McGuire, Phys. Rev. A 17, 182 (1978).
[3]R. Hoogewijs, L. Fiermans, and J. Vennik, Surf. Sci. 69, 273 (1977).
[4]E. D. Roberts, P. Weightman, and C. E. Johnson, J. Phys. C 8, 2336 (1975).
[5]E. D. Roberts, P. Weightman, and C. E. Johnson, J. Phys. C 8, L301-4 (1975).
[6]D. A. Shirley, Chem. Phys. Lett. 16, 220 (1972).
[7]D. A. Shirley, Chem. Phys. Lett. 17, 312 (1972).
[8]L. Ley, S. P. Kowalczyk, F. R. McFeely, R. A. Pollack, and D. A. Shirley, Phys. Rev. B 8, 2392 (1973).
[9]M. K. Bahl, R. O. Woodall, R. L. Watson, and K. J. Irgolic, J. Chem. Phys. 64, 1210 (1976).
[10]G. Malmsten, I. Thoren, S. Högberg, J. E. Bergmark, and S. E. Karlsson, Phys. Scr. 3, 96 (1971).
[11]P. Weightman, E. D. Roberts, and C. E. Johnson, J. Phys. C 8, 550 (1975).
[12]J. A. Bearden and A. F. Burr, Rev. Mod. Phys. 39, 125 (1967).
[13]J. P. Desclaux, At. Data Nucl. Data Tables 12, 312 (1973).
[14]J. H. Scofield, J. Electron Spectrosc. 8, 129 (1976).
[15]M. K. Bahl, R. L. Watson, and K. J. Irgolic, J. Chem. Phys. 66, 5526 (1977).
[16]C. E. Moore, *Atomic Energy Levels*, Natl. Bur. Std. (U.S.) Circ. No. 467 (U.S. GPO, Washington, D.C., 1952), Vol. 2.
[17]M. S. Banna, D. C. Frost, C. A. McDowell, and B. Wallbank, J. Chem. Phys. 68, 696 (1978).
[18]S. Svensson, N. Mårtensson, E. Basilier, P. Å. Malmqvist, U. Gelius, and K. Siegbahn, J. Electron Spectrosc. 9, 51 (1976).
[19]C. Froese-Fischer, Comput. Phys. Commun. 1, 151 (1969).
[20]R. Schulze, Z. Phys. 92, 212 (1934).
[21]O. Rosen and I. Lindgren, Phys. Rev. 176, 114 (1968).
[22]J. B. Mann, Report No. LASL-3690, Los Alamos Scientific Laboratory, 1967.
[23]M. K. Bahl and R. L. Watson, J. Electron Spectrosc. 10, 111 (1977).
[24]W. N. Asaad and W. Mehlhorn, Z. Phys. 217, 304 (1968).
[25]S. N. El Ibyari, W. N. Asaad, and E. J. McGuire, Phys. Rev. A 5, 1048 (1972).
[26]S. Hagmann, G. Hermann, and W. Mehlhorn, Z. Phys. 266, 189 (1974).
[27]F. J. McGuire, Sandia Laboratories Report Sc-RR-710075, March 1971.
[28]M. K. Bahl, R. L. Watson, and K. J. Irgolic, J. Chem. Phys. 68, 3272 (1978).
[29]S. Aksela, J. Väyrynen, and H. Aksela, Phys. Lett. A 48, 19 (1974).
[30]P. Weightman, J. Phys. C. 9, 117 (1976).
[31]P. Weightman, E. D. Roberts, and C. E. Johnson, J. Phys. C 8, 550 (1975).
[32]M. Chen, B. Crasemann, and V. O. Kostroun, Phys. Rev. A 4, 1 (1971).
[33]M. K. Bahl, R. L. Watson, and K. J. Irgolic (unpublished).
[34]L. Hedin and A. Johansson, J. Phys. B 2, 1336 (1969).
[35]R. Hoogewijs, L. Fiermans, and J. Vennik, J. Phys. C 9, L103 (1976).
[36]F. P. Larkins, At. Data Nucl. Data Tables 20, 311 (1977).
[37]T. E. Gallon and J. D. Nuttall, Surf. Sci. 53, 698 (1975).
[38]S. Aksela, J. Väyrynen, and H. Aksela, Phys. Rev. Lett. 33, 999 (1974).
[39]R. B. Shalvoy, G. B. Fischer, and P. J. Stiles, Phys. Rev. B 15, 1680 (1977).
[40]J. A. Bearden, Rev. Mod. Phys. 39, 78 (1967).